

# Deep convection in the Irminger Sea forced by the Greenland tip jet

Robert S. Pickart\*, Michael A. Spall\*, Mads Hvid Ribergaard†, G. W. K. Moore‡ & Ralph F. Milliff§

\* Woods Hole Oceanographic Institution, Woods Hole, Massachusetts 02543, USA

† Danish Meteorological Institute, Copenhagen DK-2100, Denmark

‡ University of Toronto, Ontario M5s 1A1, Canada

§ Colorado Research Associates Division, NWSA, Boulder, Colorado 80301, USA

**Open-ocean deep convection, one of the processes by which deep waters of the world's oceans are formed, is restricted to a small number of locations (for example, the Mediterranean and Labrador seas). Recently, the southwest Irminger Sea has been suggested as an additional location for open-ocean deep convection. The deep water formed in the Irminger Sea has the characteristic temperature and salinity of the water mass that fills the mid-depth North Atlantic Ocean, which had been believed to be formed entirely in the Labrador basin. Here we show that the most likely cause of the convection in the Irminger Sea is a low-level atmospheric jet known as the Greenland tip jet, which forms periodically in the lee of Cape Farewell, Greenland, and is associated with elevated heat flux and strong wind stress curl. Using a history of tip-jet events derived from meteorological land station data and a regional oceanic numerical model, we demonstrate that deep convection can occur in this region when the North Atlantic Oscillation Index is high, which is consistent with observations. This mechanism of convection in the Irminger Sea differs significantly from those known to operate in the Labrador and Mediterranean seas.**

Nearly 100 years ago it was hypothesized that most of the deep water in the North Atlantic was formed in the southwest Irminger Sea by open-ocean convection<sup>1</sup>. The surface waters of the Labrador Sea were deemed too fresh to permit wintertime overturning. Over the next few decades this idea was subject to much scrutiny, and a debate ensued in the scientific literature as to whether the Labrador Sea or the Irminger Sea was the main source of deep water to the North Atlantic. Despite evidence supporting both points of view<sup>2,3</sup>, the notion that deep convection took place east of Greenland eventually fell out of favour. Today, it is commonly accepted that the body of weakly stratified water found at mid-depth (500–1,500 m) in the North Atlantic stems entirely from the Labrador Sea—hence the term ‘Labrador Sea Water’.

Recently, compelling evidence has reawoken interest in the original hypothesis<sup>4</sup>, suggesting that a significant amount of Labrador Sea Water may be formed outside the Labrador Sea after all. If true, this means that the meridional overturning circulation of the North Atlantic has a higher level of complexity than previously thought, which needs to be taken into account when interpreting observations and diagnosing models. For example, much has been made of the rapid appearance of newly ventilated Labrador Sea Water throughout the subpolar North Atlantic in the early 1990s (refs 5, 6); a second source of convection would cause us to revise the ideas put forward to explain this. One of the main puzzles regarding convection east of Greenland is the spatial scale of the overturning, which seems to be confined to the southern portion of the Irminger Sea<sup>4</sup>. Here we show that convection in the Irminger Sea is driven by the intermittent Greenland tip jet. This small-scale atmospheric jet results in large air–sea heat flux and strong wind stress curl, which together force deep oceanic mixing.

## The Greenland tip jet

Part of the reason for the emphasis on the Labrador Sea as a convective site is the harsh wintertime atmospheric forcing there. Frigid polar air blows off the Canadian land mass as storms pass by, removing heat over a large portion of the Labrador Sea<sup>7,8</sup>. This strong buoyancy loss is depicted clearly in the National Centers for Environmental Prediction (NCEP) reanalysis global meteorological fields, which have a spatial resolution of 1–2°. By contrast, the NCEP

fields show substantially lower heat loss in the Irminger Sea<sup>9</sup>. Recently, however, attention has been focused on a phenomenon known as the Greenland tip jet, a narrow, low-level jet that periodically develops in the lee of Cape Farewell<sup>10,11</sup>. It forms when high-level northwesterly winds descend orographically on the eastern (leeward) side of Greenland and accelerate owing to conservation of Bernoulli function, drawing cold air over the southern Irminger Sea<sup>10</sup>. Until now, the frequency of such tip-jet events—and their effect on the ocean—has not been investigated.

In the winter of 1996–7, a set of field programmes was undertaken to study wintertime processes in the western North Atlantic<sup>12,13</sup>. This included the implementation of the Coupled Ocean–Atmosphere Mesoscale Prediction System (COAMPS) model<sup>14</sup>. The model was run at 45-km resolution over a domain that included the Labrador and Irminger seas, and the heat flux fields were subsequently corrected for inaccuracies in high-wind conditions using *in situ* data from the field measurements<sup>15</sup>. The COAMPS model successfully captured the tip-jet occurrences during that winter, and, in particular, one robust event from 18 to 22 February. We begin our analysis by focusing on this event (which was also the subject of a previous modelling study<sup>10</sup>), in order to familiarize the reader with the phenomenon, and to investigate the effect of the tip jet on the underlying ocean.

The COAMPS zonal 10-m wind speed and 2-m air temperature (Fig. 1a) reveal the scales of the tip jet. It spans less than 2° of latitude (which is roughly the meridional grid spacing of the NCEP global data assimilation system data set), drawing cold air over the southern Irminger Sea in a fairly narrow tongue. This small meridional scale results in very strong localized wind stress curl (Fig. 1b). Note that the asymmetry of the jet leads to stronger cyclonic curl on the northern side of the jet axis. How does the COAMPS representation of this phenomenon compare to observations? To answer this we analysed wind data from the National Aeronautics and Space Administration scatterometer (NSCAT)<sup>16</sup>. The February 1997 tip-jet event is even stronger in the satellite data, where surface wind vectors are reported at 25-km resolution. The meridional scale is the same as in the model, and the cyclonic wind stress curl is of the order of 10<sup>−4</sup> N m<sup>−3</sup> (Fig. 1c). This is nearly three orders of magnitude stronger than the large-scale wintertime wind

stress curl over the western subpolar North Atlantic. It should be noted that the same tip-jet event is nearly indiscernible in the NCEP data, appearing only briefly on 18 February. By contrast, the tip-jet signature dominates the month-long average in the high-resolution COAMPS and NSCAT fields (there are other less-intense tip-jet events that month).

The strong winds and cold temperatures of the Greenland tip jet lead to enhanced heat loss in the southern Irminger Sea along a band centred near 60°N. According to the COAMPS model, the amplitude of the flux of sensible heat + latent heat averaged over the entire event is 475 W m<sup>-2</sup>. This is comparable to the observed heat

flux during storm events in the western Labrador Sea during the same winter (when deep convection was observed<sup>15</sup>). The NCEP heat flux for the February 1997 event is only 225 W m<sup>-2</sup>, which is indistinguishable from background values. Hence, the global weather models do not capture this phenomenon. The next question is, does the Greenland tip jet develop often enough to affect the Irminger Sea over an entire winter?

### High-frequency forcing

A system of meteorological weather stations has been maintained along the coast of Greenland for several decades<sup>11</sup>, and provides the opportunity to construct a climatology of tip-jet events. We must first show, however, that these events are captured in the weather station data. The most appropriately positioned station is Prins Christian Sund (labelled P in Fig. 1), which clearly captured the February 1997 event (Fig. 2). By contrast, stations I and N, just north of Cape Farewell, showed no signs of the jet even though the same low-pressure system was measured at these locations (Fig. 2a). Station A (western Cape Farewell) showed a moderate jet signal, and station Q (northwest Cape) showed an even weaker signature. Hence the cluster of meteorological stations in southern Greenland agree with the COAMPS depiction of the February 1997 tip-jet

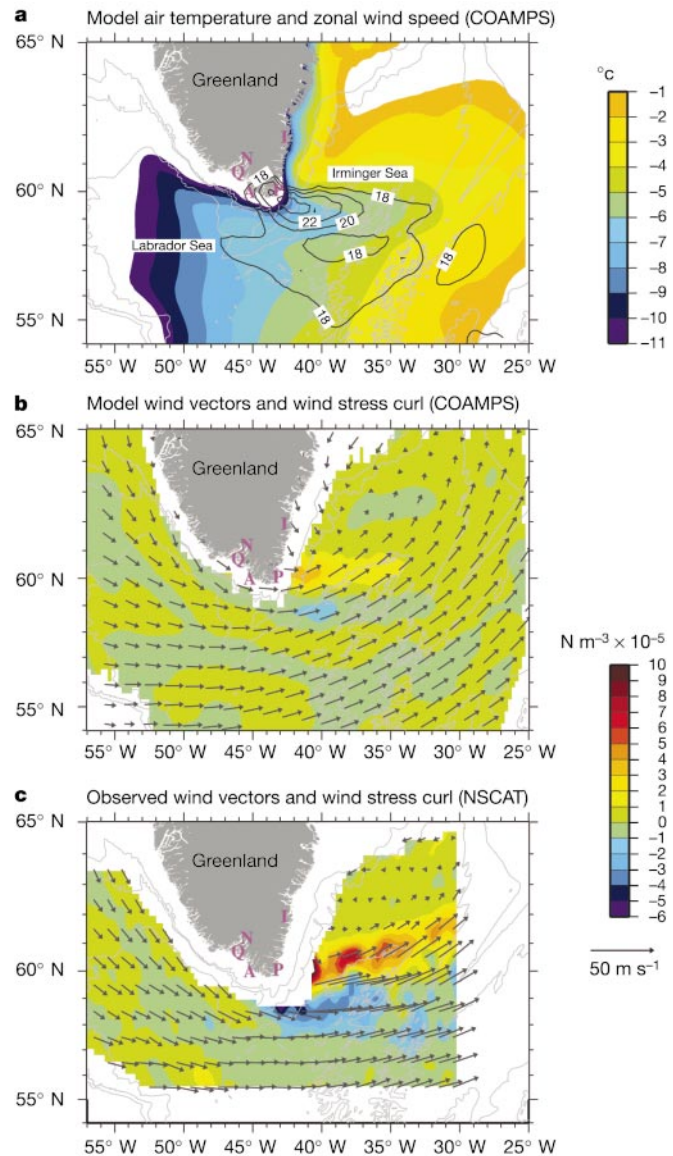


**Figure 1** The Greenland tip jet depicted by the COAMPS weather model and observed by satellite. **a**, Average 10-m zonal wind speed  $\geq 18 \text{ m s}^{-1}$  (contours), and 2-m air temperature (colour) on 18 February 1997, from COAMPS. The bottom depth contours (grey) are 1,000 m, 2,000 m and 3,000 m. The locations of the Greenland meteorological stations used in the study are denoted by the magenta lettering (P, Prins Christian Sund; A, Angisoq; Q, Qaqortoq; N, Narsarsuaq; I, Ikermiarsuk). **b**, COAMPS 10-m wind vectors and wind stress curl (colour) for 18 February 1997. Only every other wind vector is plotted. **c**, Average surface wind vectors and wind stress curl (colour) measured by NSCAT over the period 18–22 February 1997. The raw data were averaged into 0.5° bins, following previous methodology<sup>24</sup> (only bins with  $\geq 2$  realizations were used). Every other vector is plotted.

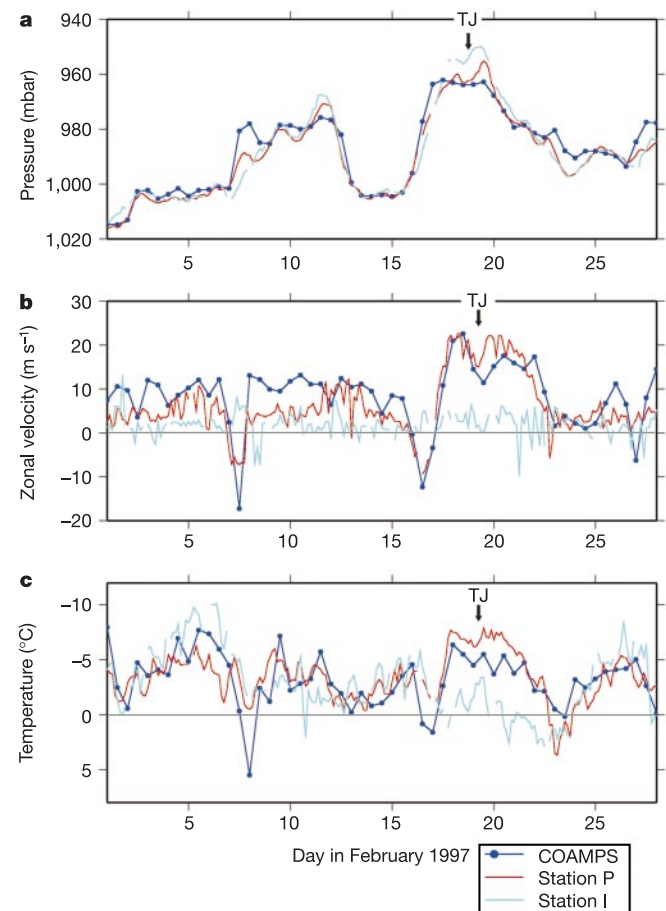


**Figure 2** A tip-jet event recorded by Greenlandic meteorological land stations. The COAMPS model output (averaged over the region 59–60°N, 37–42°W) is compared with the observed meteorological time series (see key) for February 1997. The land station data are recorded every 3 hours (gaps indicate missing data); see Fig. 1 for the locations of the meteorological stations. The tip-jet event is denoted by TJ. **a**, Sea-level pressure. **b**, Zonal 10-m wind (positive is westerly). The COAMPS and station P winds are significantly correlated ( $r = 0.72$ ); neither of them is correlated with the station I wind record. **c**, 2-m air temperature. The two meteorological station temperature records have been offset by 4° (warmer) for plotting purposes.

event, lending credence to the small meridional scale of the feature.

Inspection of the meteorological time series at station P indicates that tip-jet events are easily recognizable as bursts of strong westerly winds, accompanied by anomalously low air temperatures and sea-level pressure (for example, Fig. 2). Accordingly, we used empirical orthogonal function (EOF) analysis to identify objectively the number of tip-jet events each winter from 1962 to 1997. Maximum correlation resulted when the pressure record was lagged by 0.5 days

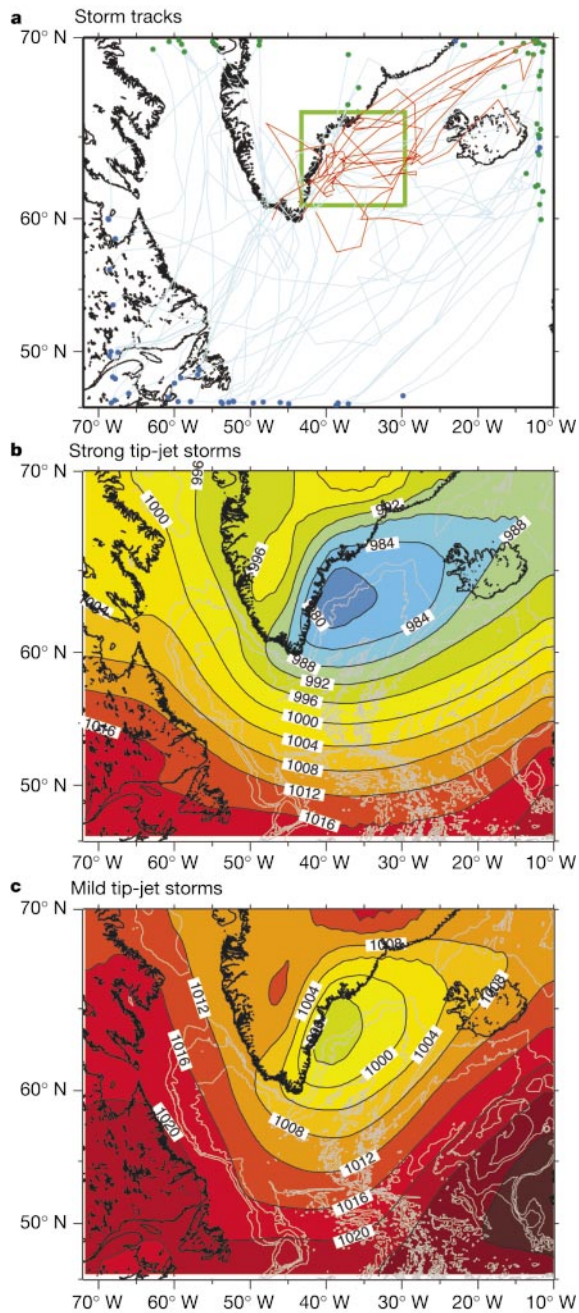


**Figure 3** Triggering of tip-jet events by passing storms. **a**, Tracks of all the low-pressure systems during winter 1993 (December–March), computed from the 6-hourly NCEP fields. A blue (green) circle denotes where the storm entered (left) the domain. The majority of the storms traversed the domain from southwest to northeast. The red-coloured portions of the tracks denote those times when the tip jet was observed at station P. The green box is the ‘trigger box’ (see text). **b**, Average NCEP sea-level pressure (mbar) for the periods when strong tip-jet storms were located in the trigger box. The bottom depth contours (grey) are 1,000 m, 2,000 m and 3,000 m. **c**, Same as **b** for the mild tip-jet storms.

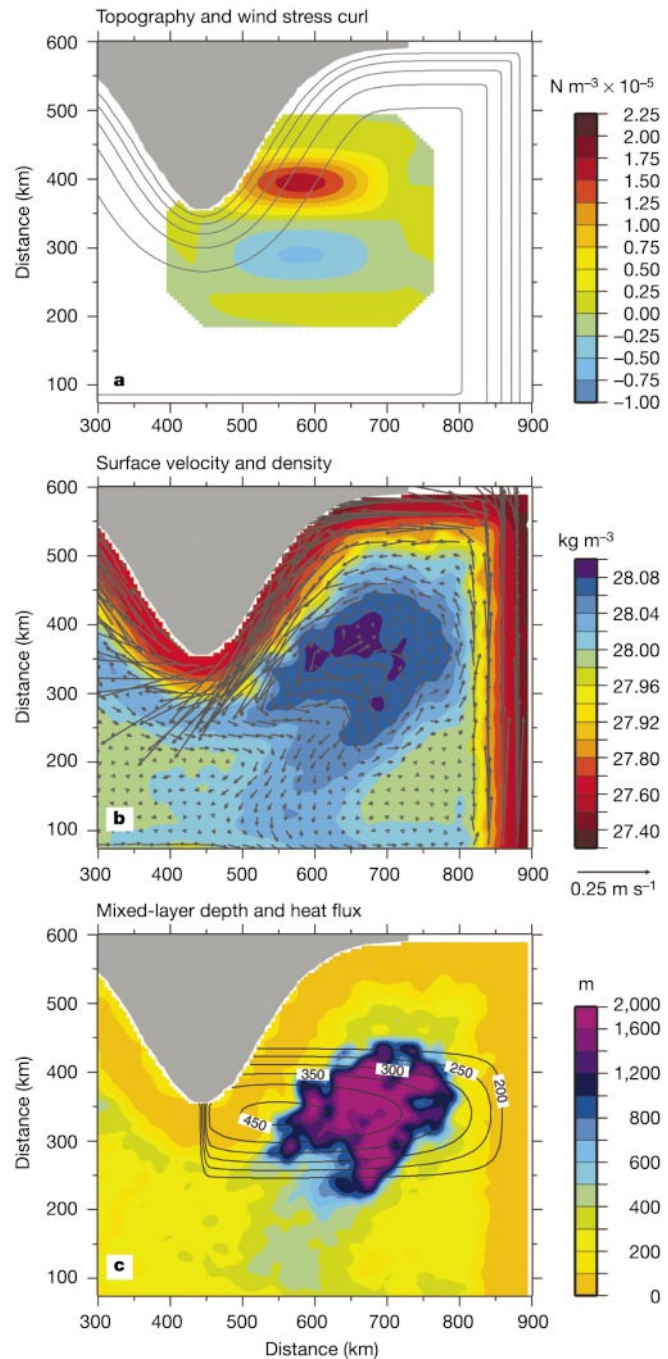


**Figure 4** Tip-jet-forced oceanic convection in a regional numerical model. **a**, Configuration and idealized wind stress curl forcing of the oceanic primitive equation model. The full domain extends from 0 to 900 km in the zonal direction, and from 0 to 600 km in the meridional direction. The horizontal resolution is 5 km, and there are 20 levels in the vertical. The bathymetric contours are 1,000–3,000 m in 500-m increments. The magnitude of the curl corresponds to the average COAMPS value over the 18–22 February 1997 tip-jet event. Although this is significantly smaller than observed by NSCAT (Fig. 1), the event was larger than normal; hence the COAMPS value is deemed more representative of typical tip-jet conditions. **b**, Surface velocity vectors (every fourth point) overlaid on surface density at the end of the second winter. The vectors represent the average over the last 30 days of the integration. Both the density and velocity were smoothed using a laplacian spline filter to remove small-scale noise. **c**, Final mixed-layer depth (smoothed as in **b**) in relation to the idealized tip-jet heat flux forcing (contours in  $\text{W m}^{-2}$ ).

(Fig. 2), and the time series were first low-passed using a 20-hour filter. The dominant EOF of the combined pressure, zonal velocity, and air temperature time series on average accounted for 55% of the total variance, more than twice that of the other two modes. This mode clearly represents the variability associated with tip-jet events. We defined a major event as one in which the reconstructed zonal EOF velocity exceeded  $9 \text{ m s}^{-1}$  (according to this criterion, the 18–22 February 1997 event was the only major one that month). Results were not sensitive to this choice—the tip-jet events stand out clearly in the original data as well as the EOFs.

We tabulated occurrences of the tip jet over the winter months (December–March) at station P. Although February tends to have more events, there is little variation throughout the winter. On average, a tip-jet event occurs roughly every 10 days, each event lasting approximately three days. The average zonal wind speed is  $12.4 \text{ m s}^{-1}$  (note that station P is upstream of the maximum jet amplitude, Fig. 1a). Thus, this phenomenon is extremely common. It is in fact one of the dominant winter weather patterns over southern Greenland (L. Rasmussen, personal communication). In addition, there is a ‘shoulder season’ in late autumn and early spring, during which additional tip-jet events often occur.

Is there a clear relationship between storms in the vicinity of Greenland and the occurrence of the tip jet? To investigate this, we tracked all the low-pressure systems during the winter of 1993 (a strong winter) using the NCEP data (which captures synoptic systems well), and compared them to the station P time series. This reveals that the tip jet tends to form when storms are situated between Cape Farewell and Iceland (Fig. 3a). In particular, all 10 events in 1993 occurred when the centre of the low-pressure system passed through the ‘trigger box’ delineated in Fig. 3a. There were seven other storms that passed through this box, and inspection of the EOF time series from station P reveals that every one of them resulted in a mild tip-jet event (that is, not strong enough to meet the criterion specified above). This is because the storms in question were not as robust (compare Fig. 3b and c). Hence there can be many tip-jet events (both strong and mild) during a robust winter; these events—apparently without exception—are triggered when a storm passes to the northeast of Cape Farewell.

Although on average there is little intra-seasonal variation in tip-jet occurrences, there is strong inter-annual variability: some years have only a few events (in fact two of the winters during the

study period had no major events). Storm activity in the subpolar North Atlantic is strongly related to the North Atlantic Oscillation (NAO) wintertime index<sup>17</sup>. A positive index is associated with a more northeasterly storm track, and so a greater number of synoptic systems pass near Greenland<sup>18</sup>. This implies that there should be a relationship between the NAO and the number of tip-jet events in a winter. Our data reveal a statistically significant correlation over the 35-year time period, with a larger index implying more frequent events. Hence, a positive NAO tends to favour the occurrence of convective overturning in the southwest Irminger Sea, as it does in the Labrador Sea<sup>19</sup>. However, tip-jet events seem to be also affected by more subtle changes in storm trajectories. In winter of 1999 the centre of action of the NAO shifted to the east<sup>20</sup>, and the trajectories of numerous storms passed farther offshore of Greenland. Although the NAO index was high for that winter, the eastward shift resulted in more moderate conditions in the Labrador Sea (and less tendency for deep convection there<sup>20</sup>). In 1999 there were 10 major tip-jet events, typical for a high-NAO winter. However, the eastward shift in storm trajectories resulted in significantly warmer air being advected over the Irminger Sea within the tip jet (on average  $4^\circ\text{C}$  warmer than for the winter of 1993). This corresponds to a reduction in the sensible heat loss of roughly  $115 \text{ W m}^{-2}$ . Hence, as for the Labrador Sea, such an anomalous NAO state is apparently less favourable for deep overturning east of Greenland as well.

### Oceanic response

To investigate the effect of tip-jet forcing on the ocean, and in particular its potential to drive deep convection in the Irminger Sea, we ran a regional application of the MIT primitive equation numerical model<sup>21</sup>. The domain, meant to correspond to the western subpolar North Atlantic, has an idealized representation of Greenland and the continental slope (Fig. 4a). The model was initialized with measured temperature and salinity profiles from the Irminger Sea, representative of the stratification in late summer found during a high-NAO year. Density is calculated from temperature and salinity using a linear equation of state. In order to include the effects of the buoyant boundary current encircling the Irminger Sea (the Irminger Current), the stratification and horizontal velocity are restored towards a narrow, surface-intensified geostrophic jet along the southern and eastern boundaries. The model boundary current follows the topographic contours cyclonically around the basin, passing along the east coast of Greenland.

We forced the model with a representation of the Greenland tip jet. The climatology indicates that for a typical high-NAO winter there are 10 major events from mid-December to mid-March. As there are often significant events in late autumn and early spring, as well as numerous mild events throughout the winter, we parameterized this by applying 14 equally strong events over 120 days (each event lasts 4 days and they are spaced 8 days apart). Results are not overly sensitive to these details. The model was initially run for one year using the wind forcing only, allowing the oceanic circulation to spin up. This provides an important pre-conditioning effect for the subsequent winter in which both wind and buoyancy forcing are applied.

We present results from the end of the second winter, during which both the tip-jet wind stress curl (Fig. 4a) and heat flux (Fig. 4c) were applied. A strong cyclonic gyre develops to the east of Cape Farewell, with a weaker anti-cyclonic swirl to the south (Fig. 4b); this is to be expected from the wind forcing. A region of increased surface density and deep mixed-layers, roughly 200 km in diameter, forms as well to the east of Cape Farewell (Fig. 4b, c). The deepest mixed layers, which took roughly 2.5 months to develop, extend to 2,000 m. This is clearly deep convection, in line with recent hydrographic observations<sup>4</sup> that indicate overturning to 1,800 m in this area. The location and size of the model convective patch agree closely with that suggested by the measured potential vorticity (PV) distribution during the high-NAO period of the

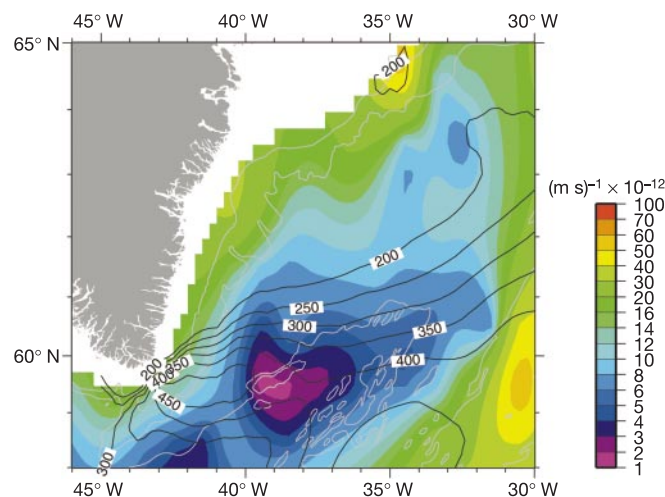


**Figure 5** Observational support for tip-jet-forced deep convection east of Greenland. The figure shows average planetary potential vorticity (colour) at 1,000 m for the period 1989–97, from a climatological database<sup>4</sup>, in relation to the COAMPS tip-jet heat flux forcing (18–22 February 1997). This represents the observational analogue of Fig. 4c. The bottom depth contours (grey) are 1,000 m, 2,000 m and 3,000 m.

1990s<sup>4</sup> (compare Figs 4c and 5). Both fields indicate a well-defined, isolated area of overturning in the southern Irminger Sea.

The wind forcing provided by the tip jet significantly affects the overturning. Strong Ekman suction decreases the thickness of the warm surface layer in the region of buoyancy loss, reducing the amount of heat required to be removed during winter. Calculations with cooling but no wind stress show that the deep convection occurs significantly later in the season, and the final volume of ventilated water is reduced by approximately 35%. An additional calculation was done in which a shallow layer of fresh water was included near the coast, representative of the East Greenland Current (initialized with a measured near-shore hydrographic profile). It produced convection to 2,000 m with a total volume nearly as large as the standard case. This insensitivity is because most of the fresh water remains trapped to the boundary, as is observed in this region<sup>4</sup>. Finally, convection reaches only 700 m when the initial density profile is representative of the stratification during low-NAO conditions. This suggests that deep overturning is unlikely to occur in low-NAO winters, or even during the first winter of strong forcing following several low-NAO years. This is consistent with the notion that the Irminger Sea has a convective memory longer than one year<sup>4</sup>.

### Importance of tip-jet-forced convection

The circumstances surrounding convection in the Irminger Sea are very different from those in the other two locations of deep overturning in the North Atlantic—the Labrador and Mediterranean seas. The Labrador Sea has broad-scale wind and buoyancy forcing over most of the basin, with no strong wind stress curl. The small spatial scale of the forcing in the Irminger Sea is more reminiscent of the Mediterranean Sea, yet there are fundamental differences. The mistral and tramontane wind events in the Mediterranean occur less often, and can last substantially longer<sup>22</sup>. Furthermore, these winds are meridional (northerly). A modelling study of the Mediterranean case—using sustained winds over several months—demonstrated that a single cyclonic gyre develops directly underneath the forcing region, within which the deepest convection occurs<sup>23</sup>. By contrast, in the Irminger Sea the zonal orientation of the (highly intermittent) tip jet spins up a dipole circulation, which resides to the east of the strongest forcing. Diagnosis of a series of model calculations indicates that this offset is due to the advection of density by the wind-driven flow. The effect of the anti-cyclonic circulation is evident by the tongue of dense water extending to the southwest (Fig. 4b), which enables deep convection to occur over a broader region (Fig. 4c). Both the model and observations show the eastward displacement of the Irminger Sea convective patch relative to the forcing.

It is important to note that we are not advocating the Irminger Sea as the sole or primary source of Labrador Sea Water. It does, however, appear to be a significant source. Although there are no direct estimates of new water production in the Irminger Sea, the volume of new water formed in the model (corresponding to the region where mixed-layer depths exceed 1,000 m) is  $4.5 \times 10^{13} \text{ m}^3$ . Using the  $PV = 5 \text{ m}^{-1} \text{ s}^{-1} \times 10^{-12}$  contour as the delimiter of newly convected water in the observations (Fig. 5), and assuming an average convective depth of 1,500 m, gives a similar estimate of  $4.6 \times 10^{13} \text{ m}^3$ . This is comparable to the measured amount of new water formed in the Labrador Sea in the winter of 1996–7 ( $4.0 \times 10^{13} \text{ m}^3$ , the only such observational estimate for the Labrador Sea). Admittedly that winter was moderate<sup>9</sup>; none the less, it suggests that the Irminger Sea source is important. Furthermore, because the convected water formed in the Irminger Sea is not

confined within the cyclonic gyre (Fig. 4), it can more readily affect the surrounding area.

The implications of an additional source of Labrador Sea Water are far-reaching. It alters our view of the mid-depth component of the North Atlantic meridional overturning circulation, and means that we need to consider both observations and modelling studies from a new perspective. Our results also provide a striking example of the coupling that can occur between high-frequency, small-scale events in the atmosphere, and low-frequency, climatically important processes in the ocean. □

Received 25 October 2002; accepted 19 March 2003; doi:10.1038/nature01729.

1. Nansen, F. Das Bodenwasser und die Abkühlung des Meeres. *Int. Rev. Ges. Hydrobiol. Hydrogr.* **V**, 1–42 (1912).
2. Wüst, G. Der subarktische Bodenstrom in der westatlantischen Mulde. *Ann. Hydrogr. Marit. Meteorol.* **IV/VI**, 249–256 (1943).
3. Nielsen, J. *Greenland. The Discovery of Greenland, Exploration, and the Nature of the Country* Vol. I, 185–230 (C.A. Reitzel, Copenhagen, 1928).
4. Pickart, R. S., Straneo, F. & Moore, G. W. K. Is Labrador Sea Water formed in the Irminger Basin? *Deep Sea Res.* **150**, 23–52 (2003).
5. Sy, A. *et al.* Surprisingly rapid spreading of newly formed intermediate waters across the North Atlantic Ocean. *Nature* **386**, 675–679 (1997).
6. Rhein, M. *et al.* Labrador Sea water: Pathways, CFC-inventory, and formation rates. *J. Phys. Oceanogr.* **32**, 648–665 (2002).
7. Bumpke, K., Karger, U. & Uhlig, K. Measurements of turbulent fluxes of momentum and sensible heat over the Labrador Sea. *J. Phys. Oceanogr.* **32**, 401–410 (2002).
8. Moore, G. W. K. & Renfrew, I. A. An assessment of the surface turbulent heat fluxes from the NCEP-NCAR reanalysis over the western boundary currents. *J. Clim.* **15**, 2020–2037 (2002).
9. Pickart, R. S., Torres, D. J. & Clarke, R. A. Hydrography of the Labrador Sea during active convection. *J. Phys. Oceanogr.* **32**, 428–457 (2002).
10. Doyle, J. D. & Shapiro, M. A. Flow response to large-scale topography: the Greenland tip jet. *Tellus* **51**, 728–748 (1999).
11. Cappelen, J., Jørgensen, B. V., Laursen, E. V., Stannius, L. S. & Thomsen, R. S. *The Observed Climate of Greenland, 1958–99, with Climatological Standard Normals, 1961–90* (Technical Report 00-18, Danish Meteorological Institute, Copenhagen, 2001).
12. Labea Group. The Labrador Sea deep convection experiment. *Bull. Am. Meteorol. Soc.* **79**, 2033–2058 (1998).
13. Browning, K. A., Chalou, J.-P. & Thorpe, A. J. The Fronts and Atlantic Storm-Track Experiment (FASTEX). *Q. J. R. Meteorol. Soc.* **125**, 3129–3617 (1999).
14. Renfrew, I. A., Moore, G. W. K., Holt, T. R., Chang, S. W. & Guest, P. Mesoscale forecasting during a field program: Meteorological support of the Labrador Sea deep convection experiment. *Bull. Am. Meteorol. Soc.* **80**, 605–620 (1999).
15. Renfrew, I. A., Moore, G. W. K., Guest, P. S. & Bumpke, K. A comparison of surface-layer heat flux and surface momentum flux observations over the Labrador Sea with ECMWF analyses and NCEP reanalyses. *J. Phys. Oceanogr.* **32**, 383–400 (2002).
16. Naderi, F. M., Freilich, M. H. & Long, D. G. Spaceborne radar measurement of wind velocity over the ocean—An overview of the NSCAT scatterometer system. *IEEE Proc.* **79**, 850–866 (1991).
17. Hurrell, J. W. Decadal trends in the North Atlantic Oscillation regional temperatures and precipitation. *Science* **269**, 676–679 (1995).
18. Rogers, J. C. Patterns of low-frequency monthly sea level pressure variability (1899–1986) and associated wave cyclone frequencies. *J. Clim.* **3**, 1364–1379 (1990).
19. Dickson, R. R., Lazier, J. R. N., Meincke, J., Rhines, P. B. & Swift, J. Long-term coordinated changes in the convective activity of the North Atlantic. *Prog. Oceanogr.* **38**, 241–295 (1996).
20. Dickson, R. R. & Meincke, J. in *Trans. ICES Symp. Hydrobiological Variability in the ICES Area, 1990–99* (ed. Turrell, William) (ICES Marine Science Symposium Series, Copenhagen, 2003).
21. Marshall, J., Hill, C., Perelman, L. & Adcroft, A. Hydrostatic, quasi-hydrostatic, and non-hydrostatic ocean modeling. *J. Geophys. Res.* **102**, 5733–5752 (1997).
22. Schott, F. *et al.* Observations of deep convection in the Gulf of Lions, Northern Mediterranean, during the winter of 1991/92. *J. Phys. Oceanogr.* **26**, 505–524 (1996).
23. Madec, G., Lott, F., Delecluse, P. & Crepon, M. Large-scale preconditioning of deep-water formation in the Northwestern Mediterranean Sea. *J. Phys. Oceanogr.* **26**, 1393–1408 (1996).
24. Milliff, R. F. & Morzel, J. The global distribution of the time-averaged wind stress curl from NSCAT. *J. Atmos. Sci.* **58**, 109–131 (2001).

**Acknowledgements** We thank L. Rasmussen for discussions about the meteorology around Greenland. The NSCAT surface winds were derived from the KU2000 retrieval provided by Remote Sensing Systems Inc. Support for this work was provided by the Ocean Sciences Division of the National Science Foundation.

**Competing interests statement** The authors declare that they have no competing financial interests.

**Correspondence** and requests for materials should be addressed to R.P. (rpickart@whoi.edu).